

***N,N'*-bis(2-(benzylthio)ethyl)malonamides: Synthesis, Electronic and Steric effects in Silver(I) Extraction and Silver(I) Binding Studies**

Abiodun D. Aderibigbe*^{1,2} and Andrew J. Clark¹

¹*Department of Chemistry, University of Warwick, Coventry CV4 7AL.*

²*Department of Chemistry, The Federal University of Technology Akure, P.M.B. 704 Akure, Ondo state, Nigeria.*

Abstract

Unsubstituted and gem-diethyl substituted malonamide derivatives, bearing benzylthio arms were prepared in moderate to high yields at room temperature. It was observed that electronics effects at the 4-aryl position in the malonamide derivatives had a significant effect on the selectivity, but little effect on silver(I) extraction efficiency measured by liquid-liquid extraction experiments (with the 4-methoxy analogue proving the most selective). Increased steric hindrance near the sulfur donor had a small negative effect on silver(I) extraction efficiency, while hindrance at the methylene centre reduces selectivity. One of the malonamide derivatives prepared was found to bind to silver(I) in a 1:1 fashion suggesting a tetrahedral coordination type.

Keywords: Malonamide derivatives, selective silver(I) extraction, electronics, sterics, Job's and mole ratio plots.

Introduction

As the world population increases, the demand for products like phones, laptops, batteries, jewellery etc., containing precious metals like silver is certain to increase as well.[1–3] Unfortunately, silver just like other metals are non-renewable resources. Therefore, in order to meet the increasing demand, the supply of silver must be guaranteed. Two major options that have been explored to guarantee the supply of silver and indeed other metals is the search for new primary sources[4], (new metal ore deposits) and the secondary sources or urban mining, in other words, recycling of metals[5]. The success of these options rests on the development of an efficient, metal selective and cost-effective Ag⁺ recovery process.

N,N'-malonamide derivatives (MADs) such as **1a** (Figure 1) have attracted attention due to their versatility for metal recovery in separation science, having demonstrated outstanding efficiency and selectivity in the recovery of highly valuable metals including lanthanides, actinides and precious metals[6–9]. The presence of two acyl groups and an active methylene centre allows the modification of the structural features of this ligand towards accessing derivatives with selective metal recovery and desired solubility properties.[9] Addition of specific donors has been shown to improve the efficiency

and selectivity of the MADs for metal recovery. For example, Daubinet and Kaye[9], prepared a range of MADs (**1a-d**) (Figure 1) with different donor groups and varying degrees of lipophilicities via a microwave-assisted method and observed that the malonamide derivative **1a** bearing a benzylthio arm demonstrated the highest efficiency (97 %) and selectivity of Ag⁺ recovery from a solution also containing Cu²⁺ and Pb²⁺.

As part of an ongoing program exploring the development of *in situ* technologies for recovery of precious metals, from waste repositories (including metallurgical slag heaps, mine tailings and possibly landfills), we queried the possibility of accessing a Ag⁺-selective ligand bearing a vinyl handle which can be tethered by polymerization to a magnetic nanoparticle. The malonamide derivative **1e**, (Figure 1) was chosen as our initial target after we had judged that it could be easily prepared and that it has high stability in low pH environments. Unfortunately, previously reported conditions for accessing the related malonamide derivative ligand **1a** involve high temperatures which we feared could occasion the polymerization of the important vinyl group. Therefore, initial study focused on the development of a room temperature method to accessing derivatives of **1a**; **1e-i** (Figure 2). Subsequently the effect of electronics (using **1a** and **1e-h**) and sterics (using **1a**, **1i** and **3a**) (Figure 2) on Ag⁺ extraction was investigated to understand how modification affects the selectivity and efficiency of the ligand. Finally, the binding stoichiometry of the Ag⁺-**1a** complex was thoroughly investigated to gain an insight into the Ag⁺ binding nature of the ligand **1a**.

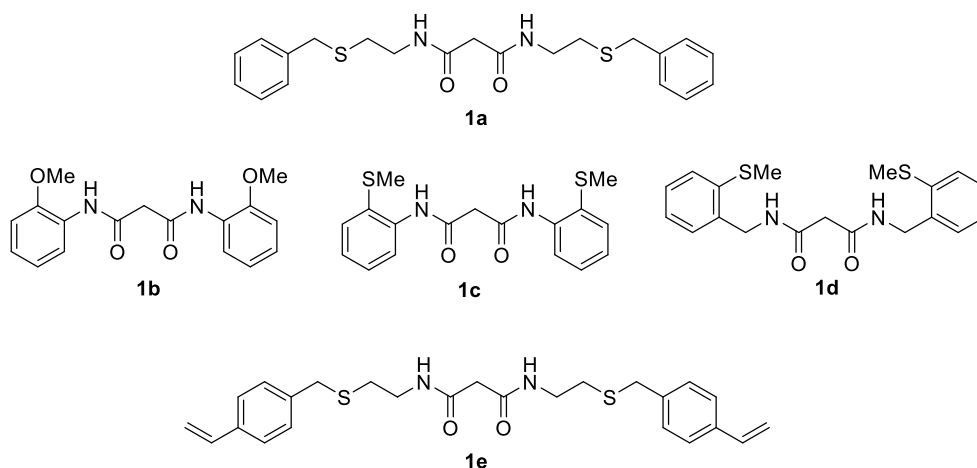


Figure 1. *N,N'*-malonamide derivatives 1a-e.

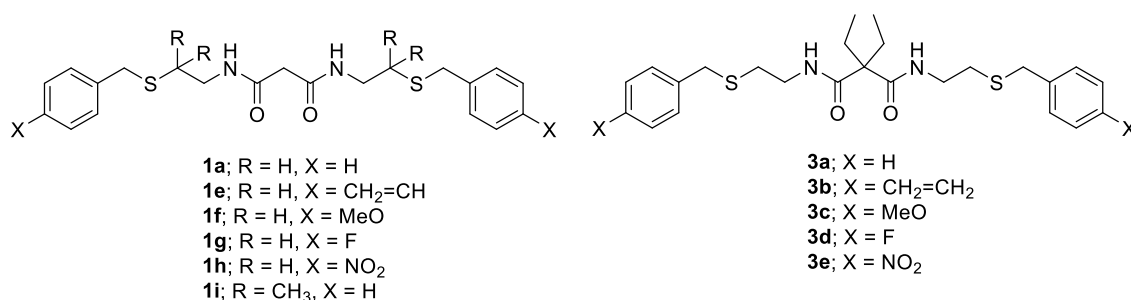


Figure 2. *N, N'*-malonamide derivatives synthesized in this work

Material and methods

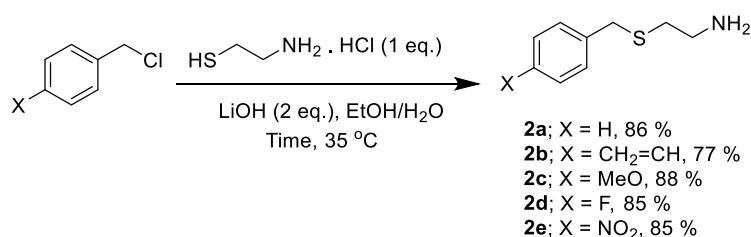
Materials and instrumentation

All reagents were purchased from commercial sources and used as received. ¹H and ¹³C NMR were recorded at room temperature on Bruker® Advance spectrometers and all chemical shift values were referenced to an internal standard of tetramethylsilane ($\delta = 0.0$ ppm). Fourier transform infra-red (FTIR) spectra were recorded on Bruker® Alpha Platinum-Attenuated Total Reflectance IR spectrometer. All accurate mass spectra were run on a Bruker® MaXis mass spectrometer. Metal concentrations were measured by means of a PerkinElmer 5300DV Inductively Coupled Plasma Optical Emission spectrophotometer (ICP-OES).

Methods

Syntheses

S-benzylcysteamines (2a - e).



Scheme 1. Syntheses of *S*-benzylcysteamines **2a-e**[10]

The benzylcysteamines **2a-e** were synthesized following the method reported by Ghosh and Tochtrop[10]. Briefly, to a stirred water/ethanol (1:3) solution of LiOH (2 eq.) and 2-aminoethanethiol hydrochloride (1 eq.) was added dropwise for 5 min, the appropriate benzyl chlorides (1 eq.) and the reaction was left to stir at 35 °C for 20 min (for **2a**) or 40 min (for **2b-e**) after which the solvent was removed *in vacuo* (Scheme 1). The crude mixture was extracted with dichloromethane (DCM) after it

had been solubilized with water. The DCM extract was then dried with anhydrous Na₂SO₄ or MgSO₄, filtered and concentrated *in vacuo*. All amines except for **2d** (the fluoro analogue) were obtained as oils needing no purification. The amine **2d** was subsequently purified by column chromatography using a mobile phase gradient of 100 % EtOAc to 50 % v/v EtOAc/MeOH.

2-((Benzylthio)ethan-1-amine (2a).[10] Viscous colourless oil. Yield: 5.76 g (86 %), $\nu(\text{cm}^{-1})$ 3363, 3279 (N-H stretch), 1600 (N-H bend), ¹H NMR (400 MHz, CDCl₃) δ 7.39 – 7.18 (m, 5H, ArH), 3.70 (s, 2H, PhCH₂S), 2.81 (t, $J = 6.5$ Hz, 2H, SCH₂CH₂), 2.51 (t, $J = 6.5$ Hz, 2H, SCH₂CH₂), 1.29 (s, 2H, CH₂CH₂NH₂), ¹³C NMR (100 MHz, CDCl₃) 138.5, 128.9, 128.6 and 127.1 (ArC), 40.9 (CH₂CH₂NH₂), 36.0 (PhCH₂S), 35.7 (SCH₂CH₂); m/z (ESI): 168 [M + H]⁺.

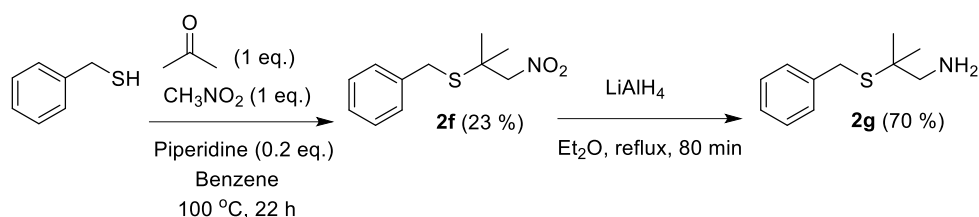
2-((4-Vinylbenzylthio)ethan-1-amine (2b). Viscous yellow oil. Yield: 5.87 g (77 %), $\nu(\text{cm}^{-1})$ 3365, (N-H stretch), 1627, 1567 (N-H bend), ¹H NMR (300 MHz, CDCl₃) δ 7.36 (d, $J = 8.0$ Hz, 2H, ArH), 7.27 (d, $J = 8.0$ Hz, 2H, ArH), 6.70 (dd, $J = 17.5, 11.0$ Hz, 1H, CH₂CHPh), 5.73 (d, $J = 17.5$ Hz, 1H, CH_aH_bCHPh), 5.23 (d, $J = 11.0$ Hz, 1H, CH_aH_bCHPh), 3.69 (s, 2H, PhCH₂S), 2.82 (t, $J = 6.0$ Hz, 2H, CH₂CH₂NH₂), 2.51 (t, $J = 6.0$ Hz, 2H, SCH₂CH₂), 1.29 (s, 2H, CH₂CH₂NH₂), ¹³C NMR (75 MHz, CDCl₃) δ 138.1 and 136.5 (ArC), 136.4 (CH₂CHPh), 129.1 and 126.5 (ArC), 113.9 (CH₂CHPh), 41.0 (CH₂CH₂NH₂), 35.8 (PhCH₂S), 35.7 (SCH₂CH₂), m/z (ESI): [M + H]⁺ for [C₁₁H₁₆NS]⁺, calculated; 194.1003, found 194.0998.

2-((4-Methoxybenzylthio)ethan-1-amine (2c).[10] Viscous colourless oil. Yield: 4.37 g (88 %), $\nu(\text{cm}^{-1})$: 3261 (N-H stretch), 1663 (N-H bend), ¹H NMR (400 MHz, CDCl₃) δ 7.23 (d, $J = 8.5$ Hz, 2H and 6.84 (d, $J = 8.5$ Hz, 2H) (ArH), 3.79 (s, 3H, CH₃OPh), 3.67 (s, 2H, PhCH₂S), 2.85 (t, $J = 6.5$ Hz, 2H, CH₂CH₂NH₂), 2.71 (s, 2H, CH₂CH₂NH₂), 2.55 (t, $J = 6.5$ Hz, 2H, SCH₂CH₂). ¹³C NMR (100 MHz, CDCl₃) δ 159.0, 130.2, 130.0 and 114.1 (ArC), 55.4 (CH₃OPh), 40.5 (CH₂CH₂NH₂), 35.4 (PhCH₂S), 34.5 (SCH₂CH₂), m/z (ESI): 198 [M + H]⁺.

2-((4-Fluorobenzylthio)ethan-1-amine (2d).[10] Viscous colourless oil. Yield: 4.27 g (85 %), $\nu(\text{cm}^{-1})$: 3365 (N-H stretch), 1599 (N-H bend), ¹H NMR (400 MHz, CDCl₃) δ 7.35 – 7.23 (dd, 2H, $J_{\text{HCCCH}} = 9$ Hz, $J_{\text{HCCCF}} = 3$ Hz, ArH), 7.06 – 6.96 (t, 2H, $J_{\text{HCCF}} = 15$ Hz, ArH), 3.68 (s, 2H, PhCH₂S), 2.82 (t, $J = 6.5$ Hz, 2H, CH₂CH₂NH₂), 2.51 (t, $J = 6.5$ Hz, 2H, SCH₂CH₂), 1.33 (s, 2H, CH₂CH₂NH₂), ¹³C NMR (100 MHz, CDCl₃) δ 162 (d, $J_{\text{CF}} = 244$ Hz), 134.2 (d, $J_{\text{CCCCF}} = 3$ Hz), 130.4 (d, $J_{\text{CCF}} = 8$ Hz) and 115.4 (d, $J_{\text{CCF}} = 21$ Hz) (ArC), 40.9 (CH₂CH₂NH₂), 35.6 (PhCH₂S), 35.2 (SCH₂CH₂), m/z (ESI): 186 [M + H]⁺.

2-((4-Nitrobenzylthio)ethan-1-amine (2e).[10] Yellow oil. Yield: 3.23 g (85 %), $\nu(\text{cm}^{-1})$: 3365 (N-H stretch), 1599 (N-H bend), 1367 (N-O stretch), ¹H NMR (300 MHz, CDCl₃) δ 8.18 (d, $J = 8.5$ Hz, 2H, ArH), 7.50 (d, $J = 8.5$ Hz, 2H, ArH), 3.79 (s, 2H, PhCH₂S), 2.85 (t, $J = 6.5$ Hz, 2H, CH₂CH₂NH₂), 2.53 (t, $J = 6.5$ Hz, 2H, SCH₂CH₂), 1.38 (s, 2H, CH₂CH₂NH₂), ¹³C NMR (75 MHz, CDCl₃) δ 147.1 (ArC), 146.4 (ArC), 129.7 (ArC), 123.9 (ArC), 40.9 (CH₂CH₂NH₂), 35.8 (PhCH₂S), 35.6 (SCH₂CH₂), m/z (ESI): 213 [M + H]⁺.

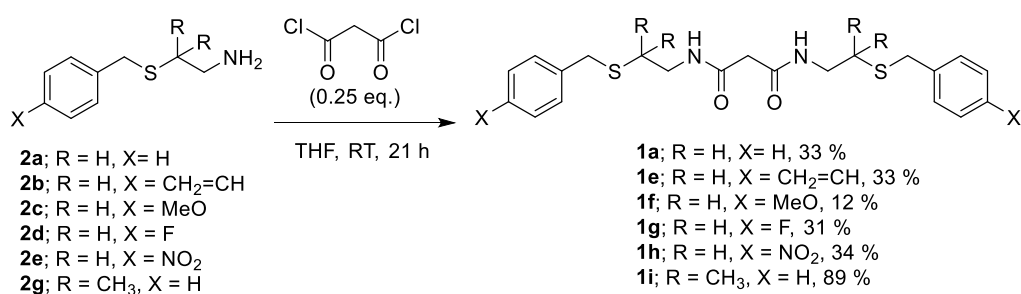
Gem-dimethyl substituted *S*-benzylcysteamine (**2g**)[11]



Scheme 2. Synthesis of the gem-dimethyl substituted *S*-benzylcysteamine **2g**[11]

Access to 2,2-dimethyl-2-benzylthioethyl amine **2g** was achieved by following the method reported by Carroll and coworkers.[11] In the first step, a mixture of acetone (3.67 ml, 0.05 mol), benzylmercaptan (5.90 ml, 0.05 mol), nitromethane (2.71 ml, 0.05 mol) and benzene (18.75 ml) were heated at 100 °C inside a flask fitted with a Dean Stark apparatus filled with benzene (Scheme 2). After 22 h, the crude mixture was left to cool and was washed with 2.0 M HCl and then with water. It was then dried with anhydrous MgSO₄, concentrated *in vacuo* and purified by flash chromatography using *n*-hexane as eluent to yield 1-(benzylthio)-1,1-dimethylnitroethane **2f** (2.60 g, 23 %). In the second step, a dry ether solution of 1-(benzylthio)-1,1-dimethylnitroethane **2f** (1 g, 4.4 mmol) was added to a cold ether solution of LiAlH₄ (4 M, 3.25 ml) inside a 2-necked flask. The mixture was left to stir for another 3 min after which it was transferred to a heating block and heated under reflux for 100 min. The crude mixture was transferred to a 250 ml flask and a stir bar added. Water and subsequently potassium sodium tartarate (25 ml, 20 %) was added. The mixture was left to stir until all solids dissolved. The crude product was then extracted with ether (20 mL x 3) and purified by flash chromatography (16 – 50 % ethyl acetate: *n*-hexane, ethyl acetate and finally methanol) to give 2-(benzylthio)-2,2-dimethylmethanamine **2f** as a yellow oil. Yield: (0.60 g, 70%), ν (cm⁻¹) 3376 (NH), ¹H (300 MHz CDCl₃) 7.40 – 7.19 (m, 5H, ArH), 3.68 (s, 2H, PhCH₂S), 2.61 (s, 2H, CH₂NH₂), 1.44 (s, 2H, NH₂), 1.28 (s, 6H, SC(CH₃)₂); ¹³C (75 MHz, CDCl₃) 138.5, 129.0, 128.7 and 127.1 (ArC), 51.8 (C(CH₃)₂CH₂NH₂), 48.9 (C(CH₃)₂CH₂NH₂), 32.8 (PhCH₂S), 26.6 (C(CH₃)₂CH₂NO₂), *m/z* (ESI): 196 [M + H]⁺.

N,N'-bis(2-benzylthio)ethyl malonamides (**1a** and **1e-i**)



Scheme 3. Syntheses of the unsubstituted malonamide derivatives **1a** and **1e-i**

To a stirred solution of the amine (1 eq) in dry THF, malonyl chloride (0.25 eq) solution in dry THF was added dropwise for 90 min. The reaction mixture was left to stir overnight (Scheme 3) and the THF solvent was removed *in vacuo* after which water was added and the crude product was extracted with EtOAc. The crude product was washed successively with HCl (2 M), NaHCO₃, water and finally brine. It was then dried over Na₂SO₄ and concentrated *in vacuo* and purified by flash chromatography (20% EtOAc/Hexane to 100% EtOAc) to give the malonamide derivatives **1a** and **1e-i**.

***N,N'*-bis(2-(benzylthio)ethyl)malonamide (1a)**[9] Yellow powder. Yield: 0.21 g (33 %), m.p.: 108 – 112 °C (lit.,[9]: 105 – 106 °C), $\nu(\text{cm}^{-1})$: 3296 (amide N-H stretch), 1647 (amide C=O bend), ¹H NMR (400 MHz, CDCl₃) δ 7.40 – 7.19 (m, 10H, ArH), 7.05 (s, 2H, CONHCH₂), 3.71 (s, 4H, PhCH₂S), 3.39 (m, 4H, NHCH₂CH₂), 3.10 (s, 2H, COCH₂CO), 2.56 (t, $J = 6.5$ Hz, 4H, CH₂CH₂S), ¹³C NMR (100 MHz, CDCl₃) δ 167.3 (COCH₂CO), 138.2, 129.0, 128.8 and 127.3 (ArC), 43.1 (COCH₂CO), 38.5 (NHCH₂CH₂), 36.0 (PhCH₂S), 30.9 (CH₂CH₂S), m/z (ESI): 425 [M + Na]⁺.

***N,N'*-bis(2-((4-vinylbenzyl)thio)ethyl)malonamide (1e)**. Yellow powder. Yield: 0.09 g (33%), m.p.: 151 – 156 °C, $\nu(\text{cm}^{-1})$: 3292 (amide N-H stretch), 1648 (amide C=O bend), ¹H NMR (400 MHz, CDCl₃) δ 7.36 (d, $J = 7.5$ Hz, 4H) and 7.27 (d, $J = 7.5$ Hz, 4H) (ArH), 6.94 (s, 2H, CONHCH₂), 6.69 (dd, $J = 17.5, 11.0$ Hz, 2H, PhCH_cCH_aH_b), 5.73 (d, $J = 17.5$ Hz, 2H, PhCHCH_aH_b), 5.24 (d, $J = 11.0$ Hz, 2H, PhCH_cCH_aH_b), 3.70 (s, 4H, PhCH₂S), 3.40 (m, CH₂CH₂NH), 3.11 (s, 2H, COCH₂CO), 2.56 (t, $J = 6.5$ Hz, 4H, SCH₂CH₂), ¹³C NMR (100 MHz, CDCl₃) δ 167.2 (COCH₂CO), 137.7 and 136.8 (ArC), 136.5 (CH₂CHPh), 129.2 and 126.6 (ArC), 114.1 (PhCHCH₂), 43.1 (COCH₂CO), 38.4 (CH₂CH₂NH), 35.7 (CH₂SCH₂), 30.8 (SCH₂CH₂), m/z (ESI): [M + Na]⁺ for [C₂₅H₂₇N₂NaO₂S₂]⁺ calculated: 477.1646, found: 477.1643.

***N,N'*-bis(2-((4-methoxybenzyl)thio)ethyl)malonamide (1f)**. Yellow solid. Yield: 0.43 g (12%), m.p.: 146 – 149 °C, $\nu(\text{cm}^{-1})$: 3337 (NH), 1650 (amide C=O bend), 1240 (C-O; aromatic ether), ¹H NMR (300 MHz, CDCl₃) δ 7.24 (d, $J = 8.5$ Hz, 4H, ArH), 6.97 (s, 2H, CH₂CH₂NH), 6.85 (d, $J = 8.5$ Hz, 4H, ArH), 3.79 (s, 6H, CH₃OPh), 3.67 (s, 4H, PhCH₂S), 3.40 (m, 4H, CH₂CH₂NH), 3.11 (s, 2H, COCH₂CO), 2.55 (t, $J = 6.5$ Hz, 4H, SCH₂CH₂), ¹³C NMR (75 MHz, CDCl₃) δ 167.2 (COCH₂CO), 158.6 (ArC), 130.1 (ArC), 130.0 (ArC), 114.2 (ArC), 55.4 (CH₃O), 43.1 (COCH₂), 38.5 (CH₂CH₂NH), 35.4 (PhCH₂S), 30.8 (SCH₂CH₂), m/z (ESI): [M + Na]⁺ for [C₂₃H₃₀N₂NaO₄S₂]⁺ calculated: 485.1545, found: 485.1539.

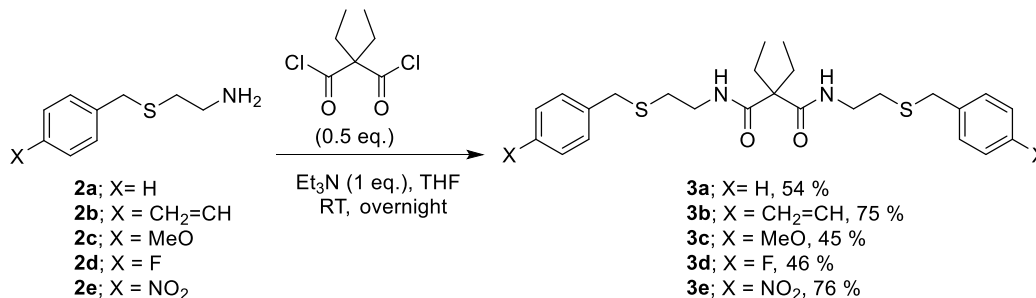
***N,N'*-bis(2-((4-fluorobenzyl)thio)ethyl)malonamide (1g)**. Yellow powder. Yield: 0.55 g (31%), m.p.: 121 – 123 °C, $\nu(\text{cm}^{-1})$: 3296 (amide N-H), 1647 (amide C=O bend), ¹H NMR (400 MHz, CDCl₃) δ 7.28 (d, $J_{\text{HCCF}} = 13.5$ Hz, 4H, ArH), 7.18 (s, 2H, CH₂NHCO), 6.99 (t, $J = 8.5$ Hz, 4H, ArH), 3.69 (s, 4H, PhCH₂S), 3.41 (m, 4H, CH₂CH₂NH), 3.15 (s, 2H, COCH₂CO), 2.55 (t, $J = 6.5$ Hz, 4H, SCH₂CH₂), ¹³C NMR (100 MHz, CDCl₃) 167.3 (COCH₂CO), 162.1 ($J_{\text{CF}} = 242$, FArC), 133.8 ($J_{\text{CCCCF}} = 3$ Hz, ArC), 130.6 and 130.5 (d, $J_{\text{CCCF}} = 8$ Hz), 115.7 and 115.5 (d, $J_{\text{CCF}} = 21$ Hz), 43.1 (COCH₂CO), 38.5

(CH₂CH₂NH), 35.2 (PhCH₂S), 30.8 (CH₂CH₂S), *m/z* (ESI): [M + Na]⁺ for [C₂₁H₂₄F₂N₂NaO₂S₂]⁺ calculated: 461.1145 found: 461.1143.

N,N'-bis(2-((4-nitrobenzyl)thio)ethyl)malonamide (**1h**). Yellow solid. Yield: 1.22 g (34%), m.p.: 82 – 85 °C, ν (cm⁻¹): 3294 (N-H stretch), 1647 (amide C=O bend), 1544 and 1367 (N-O stretch), ¹H NMR (300 MHz, CDCl₃) δ 8.17 (d, *J* = 8.5 Hz, 4H, ArH), 7.50 (d, *J* = 8.5 Hz, 4H, ArH), 7.19 (s, 2H, CH₂CH₂NH), 3.80 (s, 4H, PhCH₂S), 3.43 (m, 4H, CH₂CH₂NH), 3.16 (s, 2H, COCH₂CO), 2.58 (t, *J* = 6.5 Hz, 4H, SCH₂CH₂). ¹³C NMR (75 MHz, CDCl₃) δ 167.3, (COCH₂), 147.2 (ArC), 145.9 (ArC), 129.9 (ArC), 124.0 (ArC), 42.9 (COCH₂), 38.4 (CH₂CH₂NH), 35.4 (PhCH₂S), 31.0 (SCH₂CH₂), *m/z* (ESI): [M + Na]⁺ for [C₂₁H₂₄N₄NaO₆S₂]⁺ calculated: 515.1035, found: 515.1029.

N,N'-bis(2-(benzylthio)-2-methylpropyl)malonamide (**1i**). Cream solid. Yield: 0.68 g (89 %), m.p.: 71 – 74 °C, ν (cm⁻¹): 3260 (amide N-H stretch), 1663 (amide C=O bend), ¹H NMR (300 MHz, CDCl₃) δ 7.40 – 7.20 (m, 10H, ArH), 7.01 (s, 2H, CH₂NHCO), 3.71 (s, 4H, PhCH₂S), 3.32 (d, *J* = 6.0 Hz, 4H, C(CH₃)₂CH₂NH), 3.11 (s, 2H, COCH₂CO), 1.29 (s, 12H, SC(CH₃)₂CH₂), ¹³C NMR (75 MHz, CDCl₃) δ 167.3 (NHCOCH₂), 138.3 129.0, 128.8 and 127.2 (ArC), 48.0 (CH₂NHCO), 46.6 (PhCH₂S), 43.2 (COCH₂CO), 33.1 (SC(CH₃)₂), 26.8 (SC(CH₃)₂), *m/z* (ESI): [M + Na]⁺ for [C₂₅H₃₄N₂NaO₂S₂]⁺ calculated: 481.1959 found: 481.1959.

Gem-diethyl substituted *N,N'*-bis(2-benzylthio)ethylmalonamide derivatives (**3a-e**)



Scheme 4. Syntheses of the gem diethyl substituted malonamide derivatives **3a-e**

To a stirred solution of amine (1 eq.) and triethylamine (1 eq.) in dry diethyl ether was added a dry diethyl ether solution of diethyl malonyl chloride (0.5 eq) dropwise for 90 min. The reaction mixture was left to stir overnight (Scheme 4) after which water was added, and the crude product was extracted using diethyl ether. The organic extract was washed successively with HCl (2 M), NaHCO₃, water and brine after which it was dried over Na₂SO₄ and concentrated *in vacuo*. The crude product was purified by flash chromatography (20% EtOAc/Hexane to 100% EtOAc) to give the diethylmalonamide derivatives **3a-e**.

N,N'-Bis(2-(benzylthio)ethyl)-2,2-diethylmalonamide (**3a**). Viscous colourless oil. Yield: 1.1 g (54%), ν (cm⁻¹): 3326 (amide N-H stretch), 1630 (amide C=O bend), ¹H NMR (300 MHz, CDCl₃) δ 7.42 (s, 2H, CONHCH₂), 7.38 – 7.12 (m, 10H, ArH), 3.72 (s, 4H, SCH₂Ph), 3.41 (m, 4H, NHCH₂CH₂), 2.57 (t,

$J = 6.5$ Hz, 4H, $\text{CH}_2\text{CH}_2\text{S}$), 1.85 (q, $J = 7.0$ Hz, 4H, CCH_2CH_3), 0.82 (t, $J = 7.0$ Hz, 6H, CCH_2CH_3), ^{13}C NMR (75 MHz, CDCl_3) δ 173.2 ($\text{COC}(\text{CH}_2\text{CH}_3)_2\text{CO}$), 138.2, 129.0, 128.7 and 127.3 (ArC), 58.3 ($\text{COC}(\text{C}_2\text{H}_5)\text{CO}$), 38.2 ($\text{NHCH}_2\text{CH}_2\text{S}$), 35.9 ($\text{CH}_2\text{CH}_2\text{S}$), 31.1 (SCH_2Ph), 30.3 (CCH_2CH_3), 9.6 (CCH_2CH_3). m/z (ESI): $[\text{M} + \text{H}]^+$ for $[\text{C}_{29}\text{H}_{35}\text{N}_2\text{O}_2\text{S}_2]^+$ calculated: 459.2140 found: 459.2138.

***N,N'*-Bis(2-((4-vinylbenzyl)thio)ethyl)-2,2-diethylmalonamide (3b)**. Colourless gel. Yield: 0.12 g, (83%), $\nu_{\text{max}}(\text{cm}^{-1})$: 3323 (amide N-H stretch), 1655 (amide C=O bend), ^1H NMR (300 MHz, CDCl_3) δ 7.36 (d, $J = 7.5$ Hz, 4H, ArH and CH_2NHCO), 7.27 (d, $J = 7.5$ Hz, 4H, ArH), 6.69 (dd, $J = 17.5$, 11 Hz, 2H, $\text{CH}_2\text{CH}_2\text{Ph}$), 5.73 (d, $J = 17.5$ Hz, 2H, $\text{CH}_a\text{H}_b\text{CHPh}$), 5.23 (d, $J = 11.0$ Hz, 2H, $\text{CH}_a\text{H}_b\text{CHPh}$), 3.71 (s, 4H, $\text{CH}_2\text{CHPhCH}_2\text{S}$), 3.43 (m, 4H, $\text{CH}_2\text{CH}_2\text{NH}$), 2.57 (t, $J = 6.5$ Hz, 4H, SCH_2CH_2), 1.85 (q, $J = 7.5$ Hz, 4H, $\text{COC}(\text{CH}_2\text{CH}_3)_2$), 0.82 (t, $J = 7.5$ Hz, 6H, $\text{COC}(\text{CH}_2\text{CH}_3)_2$), ^{13}C NMR (75 MHz, CDCl_3) δ 173.2 ($\text{COC}(\text{CH}_2\text{CH}_3)_2\text{CO}$), 137.8 and 136.7 (ArC), 136.5 (CH_2CHPh), 129.2 and 126.6 (ArC), 114.0 (CH_2CHPh), 58.3 ($\text{COC}(\text{CH}_2\text{CH}_3)_2$), 38.2 (CONHCH_2), 35.6 ($\text{CH}_2\text{CHPhCH}_2\text{S}$), 31.1 ($\text{C}(\text{CH}_2\text{CH}_3)_2$), 30.3 (SCH_2CH_2), 9.6 ($\text{C}(\text{CH}_2\text{CH}_3)_2$), m/z (ESI): $[\text{M} + \text{H}]^+$ for $[\text{C}_{29}\text{H}_{36}\text{N}_2\text{O}_2\text{S}_2]^+$ calculated: 511.2453 found: 511.2450.

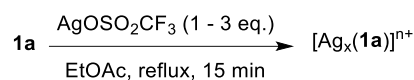
***N,N'*-Bis(2-((4-methoxybenzyl)thio)ethyl)-2,2-diethylmalonamide(3c)**. Viscous colourless oil. Yield: 1.27g (45%), ν (cm^{-1}): 3337 (NH), 1650 (amide C=O bend), 1240 (C-O; aromatic ether), ^1H NMR (300 MHz, CDCl_3) δ 7.44 (s, 2H, $\text{CH}_2\text{CH}_2\text{NH}$), 7.23 (d, $J = 8.5$ Hz, 4H, ArH), 6.84 (d, $J = 8.5$ Hz, 4H, ArH), 3.79 (s, 6H, CH_3O), 3.68 (s, 4H, PhCH_2S), 3.42 (m, 4H, $\text{CH}_2\text{CH}_2\text{NH}$), 2.56 (t, $J = 6.5$ Hz, 4H, SCH_2CH_2), 1.86 (q, $J = 7.5$ Hz, 4H, CCH_2CH_3), 0.83 (t, $J = 7.5$ Hz, 6H, CCH_2CH_3), ^{13}C NMR (75 MHz, CDCl_3) δ 173.2 (NHCO), 158.8 (ArC), 130.1 (ArC), 130.0 (ArC), 114.1 (ArC), 58.3 (COCCO), 55.4 (OCH_3), 38.2 (NHCH_2CH_2), 35.3 (SCH_2Ph), 31.0 (CCH_2CH_3), 30.2 ($\text{CH}_2\text{CH}_2\text{S}$), 9.5 (CCH_2CH_3), m/z (ESI): $[\text{M} + \text{Na}]^+$ for $[\text{C}_{27}\text{H}_{38}\text{N}_2\text{NaO}_4\text{S}_2]^+$ calculated: 518.2171, found: 541.2165.

***N,N'*-Bis(2-((4-fluorobenzyl)thio)ethyl)-2,2-diethylmalonamide (3d)**. Viscous yellow oil. Yield: 0.91 g (46%), $\nu(\text{cm}^{-1})$: 3296 (amide N-H), 1647 (amide C=O bend), ^1H NMR (300 MHz, CDCl_3) δ 7.42 (s, 2H, CH_2NHCO), 7.29 (t, $J = 8.0$ Hz, 4H, ArH), 7.00 (t, $J = 8.0$ Hz, 4H, ArH), 3.70 (s, 4H, SCH_2Ph), 3.44 (m, 4H, NHCH_2CH_2), 2.56 (t, $J = 6.0$ Hz, 4H, $\text{CH}_2\text{CH}_2\text{S}$), 1.87 (q, $J = 7.0$ Hz, 4H, CCH_2CH_3), 0.83 (t, $J = 7.0$ Hz, 6H, CCH_2CH_3). ^{13}C NMR (75 MHz, CDCl_3) δ 173.2 (COCCO), 162.1 (d, $J_{\text{CF}} = 242$, ArC), 133.9 (d, $J_{\text{CCCCF}} = 3$ Hz, ArC), 130.5 (d, $J_{\text{CCCF}} = 8$ Hz), 115.6 (d, $J_{\text{CCF}} = 21$ Hz), 58.3 (COCCO), 38.2 (NHCH_2CH_2), 35.1 (SCH_2ArC), 31.1 (CCH_2CH_3), 30.3 ($\text{CH}_2\text{CH}_2\text{S}$), 9.6 (CCH_2CH_3). m/z (ESI): $[\text{M} + \text{Na}]^+$ for $[\text{C}_{25}\text{H}_{32}\text{F}_2\text{N}_2\text{NaO}_2\text{S}_2]^+$ calculated; 517.1771 found; 517.1765.

***N,N'*-2,2-Diethyl-bis(2-((4-nitrobenzyl)thio)ethyl)malonamide (3e)**. Viscous yellow oil. Yield: 2.84 g (76%), $\nu(\text{cm}^{-1})$: 3294 (N-H stretch), 1647 (amide C=O bend), 1544 and 1367 (N-O stretch), ^1H NMR (300 MHz, CDCl_3) δ 8.18 (d, $J = 8.5$ Hz, 4H, ArH), 7.51 (d, $J = 8.5$ Hz, 4H, ArH), 7.45 (s, 2H, $\text{CH}_2\text{CH}_2\text{NH}$), 3.81 (s, 4H, PhCH_2S), 3.46 (m, 4H, SCH_2CH_2), 2.57 (t, $J = 6.5$ Hz, 4H, SCH_2CH_2), 1.87 (q, $J = 7.5$ Hz, 4H, CCH_2CH_3), 0.83 (t, $J = 7.5$ Hz, 6H, CCH_2CH_3), ^{13}C NMR (75 MHz, CDCl_3) δ 173.3

(NH \overline{C} OC), 147.2 (ArC), 146.0 (ArC), 130.0 (ArC), 124.0 (ArC), 58.3 (CO \overline{C} CO), 38.2 (CH $\overline{2}$ CH $\overline{2}$ NH), 35.3 (Ph \overline{C} H $\overline{2}$ S), 31.3 (C \overline{C} H $\overline{2}$ CH $\overline{3}$), 30.5 (S \overline{C} H $\overline{2}$ CH $\overline{2}$), 9.6 (CCH $\overline{2}$ CH $\overline{3}$), *m/z* (ESI): [M + Na]⁺ for [C₂₅H₃₂N₄NaO₆S₂]⁺ calculated: 571.1661, found 571.1605.

Silver complexes [Ag(1a)]OSO₂CF₃ (4a-c)



Scheme 5. Synthesis of Ag⁺- 1a complexes **4a-c**

The Ag⁺-**1a** complexes **4a-c** were accessed following the method reported by Daubinet.[12] Briefly, **1a** (1 eq.) was dissolved in EtOAc (5 ml) and added to AgOSO₂CF₃ (1, 2 or 3 eq.) also in EtOAc (5 ml) and heated at reflux for 15 min (Scheme 5). The product was concentrated *in vacuo* and, samples suitable for mass spectrometry analysis were prepared.

[Ag(1a)]OSO₂CF₃ (4a-c)

4a: Brown paste. Yield: 30 mg (91 %), **4b:** Brown solid. Yield: 30 mg (65 %), **4c:** Yellow paste. Yield: 50 mg (85 %). *m/z* (ESI): [M + Ag]⁺ calculated for [C₂₁H₂₆AgN₂O₂S₂]⁺; 509.0487 found; 509.0481.

Selective Ag⁺ extraction studies[13]

A solution of equal concentration of Cu²⁺, Ag⁺ and Pb²⁺ (4 ppm each) in 0.023 M Na₂SO₄ in 0.476 M HNO₃ was prepared from a 500 ppm stock solution. Chloroform was presaturated with twice its volume of 0.5 M H₂SO₄ by constant shaking in a separatory funnel for 5 min. The chloroform was used to prepare the malonamide derivative ligand solutions with molarity equal to 250 times that of Ag⁺ were prepared. For each metal extraction experiment, equal volumes (10 ml) of the metal solution and the ligand solution were contacted by rapid and vigorous stirring (using a stir bar) for 15 min in a capped plastic vial partially immersed in an oil bath set at 25 °C. Each experiment was undertaken in duplicate. After stirring, the immiscible solutions were transferred to a separatory funnel, allowed to separate and collected separately. The aqueous layer was collected into a beaker and the residual chloroform was removed over a steam bath in about 15 min. Then the aqueous layer was made back up to 10 ml and prepared for ICP-OES analysis. The metal extraction efficiencies were determined using;

$$\% EE = \frac{C_i - C_f}{C_i} \times 100$$

1

Where % *EE* is the percentage extraction efficiency, *C_i* and *C_f* are the initial and final metal ion concentrations respectively.

The selectivity of the ligands for Ag⁺ relative to Cu²⁺ and Pb²⁺ was determined as follows[14];

$$K_{Ag^+/M^{n+}} = \frac{D_{Ag^+}}{D_{M^{n+}}} \quad 2$$

Where $K_{Ag^+/M^{n+}}$ represents the selectivity coefficient of Ag^+ relative to M^{n+} ($M^{n+} = Cu^{2+}$ or Pb^{2+}), D is the distribution coefficient of the metal ions between the aqueous and the organic phases defined as;

$$D_{M^{n+}} = \frac{C_i - C_f}{C_f} \times \frac{V_{aq}}{V_{org}} \quad 3$$

$D_{M^{n+}}$ represents the distribution coefficient for the metal ion M^{n+} , C_i and C_f are initial and the final metal ion concentrations, V_{aq} and V_{org} are the volumes of the aqueous and the organic solutions respectively.

Since equal volumes of the aqueous and the organic solutions were used, the distribution factor formula was simplified into;

$$D_{M^{n+}} = \frac{C_i - C_f}{C_f} \quad 4$$

Job's plot for the 1H NMR titration of $AgClO_4$ against **1a**. [15]

Standard solutions of equal concentrations (0.005 M) of ligand **1a** and $AgClO_4$ were prepared separately in d_6 -DMSO. Varying ratios of each solution (**1a** and $AgClO_4$) were then taken and mixed together (with the overall concentration remaining the same) to target different Ag^+ mole fractions (χ_{Ag^+}). For example, to target a $\chi_{Ag^+} = 0.1$, a 0.45 ml **1a** solution was mixed with a 0.05 ml $AgClO_4$ solution inside an amber-colored NMR tube. Also, to target a $\chi_{Ag^+} = 0.2$, a 0.40 ml **1a** solution was mixed with a 0.10 ml $AgClO_4$ solution and so on until a $\chi_{Ag^+} = 0.9$ was prepared by mixing a 0.05 ml **1a** solution with a 0.45 ml $AgClO_4$ solution. The 1H NMR experiments of all mixtures and the free ligand **1a** were recorded. The plot of $\chi_{1a} \cdot \Delta\delta$ (where χ_{1a} = mole fraction of **1a** and $\Delta\delta$ = chemical shift of Ag^+ -**1a** complex minus chemical shift of free **1a**) against χ_{Ag^+} was constructed from the data generated.

Mole ratio plot for the 1H NMR titration of $AgClO_4$ against **1a**[15]

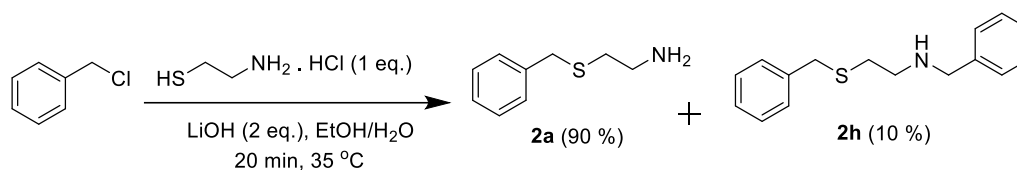
The ligand **1a** (13 mg, 0.03 mmol) was dissolved in 0.5 ml d_6 -DMSO and transferred into an amber-colored NMR tube. Standard solution of $AgClO_4$ (0.539 M) was made up in d_6 -DMSO and constant volume (30 μ L) of the $AgClO_4$ solution was added to **1a** in the NMR tube to target varying Ag^+ /**1a** mole ratios ($n_{Ag^+}/n_{1a} = 0.5$ to 4.0). For example, to target a $n_{Ag^+}/n_{1a} = 0.5$, a 30 μ L of the $AgClO_4$ solution was added using a glass syringe to the neat **1a** solution and the 1H NMR spectrum was recorded. Also, to target a $n_{Ag^+}/n_{1a} = 1.0$, a 30 μ L $AgClO_4$ solution was added to the $AgClO_4$ -**1a** with $n_{Ag^+}/n_{1a} = 0.5$ and the 1H NMR spectrum was recorded. The constant addition of the $AgClO_4$ solution was continued until

a $n_{\text{Ag}^+}/n_{\mathbf{1a}} = 4.0$ was achieved. The plot of $\Delta\delta$ (where $\Delta\delta =$ chemical shift of Ag^+ -**1a** complex minus chemical shift of free **1a**) against $n_{\text{Ag}^+}/n_{\mathbf{1a}}$ was constructed using the data generated.

Results and Discussion

Syntheses of *S*-benzylcysteamines (**2a-e**) and gem-disubstituted *S*-benzylcysteamine **2g**

The *S*-benzylcysteamines **2a-e**, were accessed following a modified protocol to that reported by Ghosh and Tochtrop.[10] For the amine **2a**, it was necessary to shorten the reaction time from 40 minutes to 20 minutes in order to minimize the formation of the dibenzylated product **2h**.



Scheme 6. Syntheses of *S*-benzylcysteamine **2a** showing the dibenzylated product **2h**

However, for the other amines **2b-e** it was necessary to extend the reaction time to 40 min to give good selectivity (< 3 % dibenzylated products observed as evidenced from ¹H NMR). Using these reaction durations (20 min for **2a** and 40 min for **2b-e**) the desired compounds apart from **2d** were prepared without the need for further purification (as evidenced by their ¹H NMR spectra). These amines served as starting material for the synthesis of the malonamide derivatives **1a** and **1e-h**.

In order to assess the effect of sterics on potential novel malonamide derived ligands, the substituted *S*-benzylcysteamine **2g** was synthesized by a modification of a method reported by Carroll *et al.*[11]. The poor yield (23 %) obtained for **2g** was attributed to the loss of acetone, during the reaction

In the original published procedure by Daubinet and Kaye[9], access to the ligand **1a** required a reaction duration of 7 days, at the end of which a yield of 24% was obtained. We prepared the ligand **1a** in less than 1 day with an improved yield of 33% through an alternative pathway involving the dropwise addition of 1 equivalent of malonyl chloride to 4 equivalents of the amine **2a** in dry THF. Related ligands **1e-i** were accessed (in low to high yields) using the same protocol.

The gem-diethyl malonamide derivatives **3a-e** were obtained in much better yields (46 – 75 %) than those obtained for the unsubstituted malonamide derivatives (**1a** and **1e-i**), presumably due to removal of competing enolisation pathways that would lower the yields.

Ag⁺ extraction studies – electronic and steric effects

Extraction studies in chloroform following the method reported by Sole and Hiskey[13] were carried out to assess the selectivity and efficiency of Ag⁺ extraction by the malonamide derived ligands **1a**, **1e-**

h and **3a** prepared. Prior to its use in preparation of the ligand solutions, the chloroform solvent was presaturated with twice its volume of an acidified deionized water to remove any water-soluble components in order to minimize volume changes during the liquid/liquid metal extraction process. An aqueous solution containing 4 ppm each of Ag^+ , Cu^{2+} and Pb^{2+} in 0.0232 M NaNO_3 was prepared by dilution of a stock solution. The choice of Cu^{2+} and Pb^{2+} as competing ions for the efficiency and selectivity extractions is borne out of the knowledge that these metals usually coexist with Ag^+ in ores and mine tailings, for instance.[16]. We decided to prepare mixed metal aqueous solutions with very low concentrations (4 ppm) of Ag^+ , Cu^{2+} and Pb^{2+} because Ag^+ typically exists in very low concentrations in Ag^+ repositories where our novel malonamide derived ligands may be applied.[16] Furthermore, NaNO_3 was added to maintain the ionic strength of the aqueous phase during extraction. For sensible comparisons to be made, each solvent extraction experiment was undertaken in duplicate and with vigorous stirring (using a stir bar with equal volumes of ligand and metal solutions for 15 mins). The concentration of the metals in the raffinate was measured by means of ICP-OES and each metal concentration value from the ICP-OES was the average of three analytic runs.

Control study

A control experiment was undertaken with the metal solution using the chloroform solvent without any ligand present. This would determine any extraction efficiency of the solvent itself (the background extraction). Interestingly, we observed that the neat chloroform itself (the control) was able to extract some metals with a slight preference for Ag^+ (Figure 3). This is likely due to the differential partial solubility of these metals in chloroform. Notwithstanding, the extraction efficiency of the ligand **1a** for Ag^+ was significantly higher than that of the neat chloroform (Figure 3), underlining the importance of the ligand **1a** in efficient Ag^+ extraction.

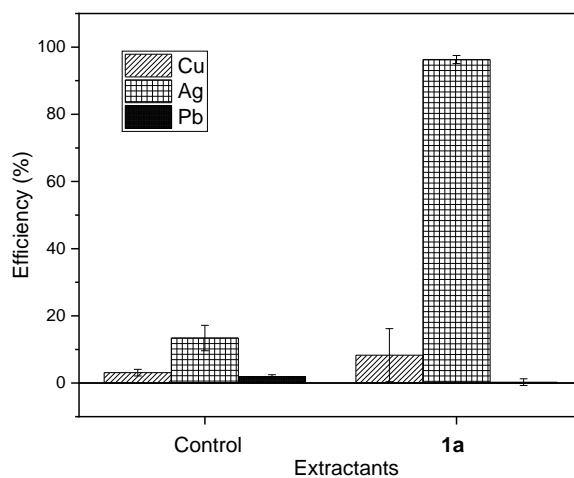


Figure 3. ICP-OES data showing metal extraction efficiencies by the neat chloroform (control) and the malonamide derived ligand **1a**

Electronics effect

The effect of electronic differences in the aryl grouping of the malonamide derived ligands on the efficiency of Ag^+ recovery was studied by comparing extraction efficiencies and selectivity's exhibited by the ligands **1a** and **1e-h**. The observed extraction efficiencies are presented in Figure 4.

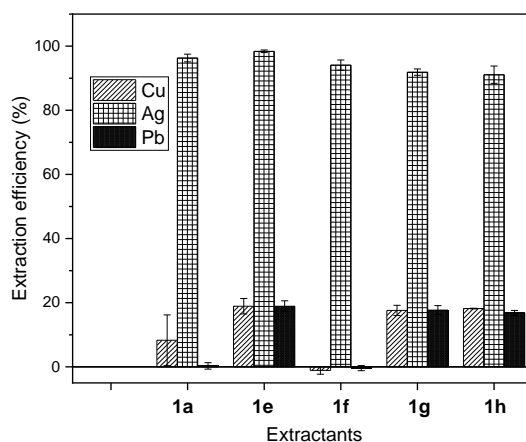


Figure 4. ICP-OES data showing metal extraction efficiencies by the malonamide derived ligands **1a**, **1e-h**

While the efficiencies for Ag^+ extraction by these ligands differ only slightly; **1a** = 96.3 ± 1.2 %, **1e** = 98.4 ± 0.4 %, **1f** = 94.1 ± 1.6 %, **1g** = 91.1 ± 1.0 %, **1h** = 91.1 ± 2.7 % (Figure 4) extraction efficiencies for those with electron withdrawing substituents **1g** and **1h** are the lowest (extraction efficiency order **1h** = **1g** < **1f** < **1a** < **1e**) (Table 1). The highest extraction efficiency observed for **1e** could be because it would give the least polar Ag^+ complex and thus have the highest solubility in chloroform.[17] Correspondingly, the least extraction efficiencies were observed for **1g** (X = F) and **1h** (X = NO_2) because (a) the Ag^+ complexes are the most polar and so less soluble in chloroform[17] and (b) the electron withdrawing nature of the aryl groups may have made the sulfur atom lone pairs less available for binding for Ag^+ (the soft sulfur atom being crucial in efficiency and selectivity following the HSAB rule).[18] For the methoxy analogue **1f** a combination of the polar nature of the Ag^+ complex lowering extraction efficiency with the more electron rich nature of the sulfur atom increasing binding leads to an intermediate extraction efficacy. The latter explanation (b), if true, would also explain the poorer selectivity's of the ligands with electron withdrawing groups (**1e**, **1g**, **1h**), noting that in the styryl analogue **1e** the inductive electron withdrawing nature of the vinyl group will be the dominant effect.

A greater selectivity would be predicated and is in fact observed for the strongly electron donating methoxy substituent in **1f**, where selectivity versus Cu^{2+} is approximately nine times better than **1a**. The results observed here suggest that electronics have only a small influence on the efficiency of Ag^+ extraction by these ligands but a significant effect on selectivity.

Table 1. Efficiency and selectivity of malonamide derived ligands **1a**, **1e-h** for Ag^+ relative to Cu^{2+} and Pb^{2+}

Ligand	Efficiency (%)	$K_{\text{Ag}^+/\text{Cu}^{2+}}$	$K_{\text{Ag}^+/\text{Pb}^{2+}}$
1a	96.3±1.2	11.6	321
1e	98.4±0.4	5.2	5.2
1f	94.1±1.6	85.5	235.3
1g	91.1±1.0	5.2	5.2
1h	91.1±2.7	5.0	5.4

Steric effect

The effect of steric hindrance at various sites in the malonamide derived ligands was investigated. Steric hindrance around the crucial sulphur atom required for binding in ligand **1i** might be predicted to lead to lower efficiencies in extraction while placing steric hindrance further away at the central carbon represented by ligand **3a**, might be predicted to have less effect (Figure 5).

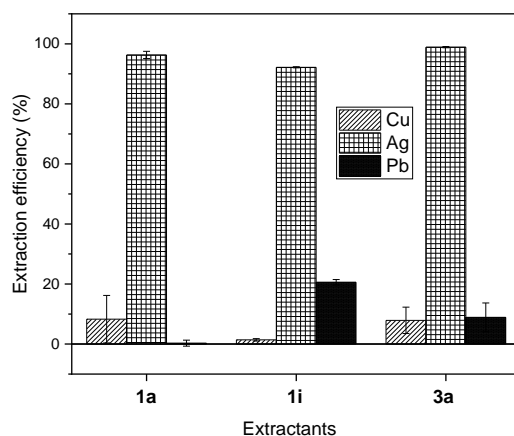


Figure 5. ICP-OES data showing metal extraction efficiencies by malonamide derived ligands **1a**, **1i** and **3a**

Ligand **1i**, sterically hindered near the sulfur atom, extracted with less efficiency (~4 %) for Ag^+ (92.2±0.2 %) than the analogue without such steric hindrance **1a** (96.3±1.2 %), (Figure 5) as predicted.

This is attributed to the slightly greater difficulty of **1i** in assuming the right conformation needed to bind Ag^+ because of the presence of the dimethyl substitution.[19] On the other hand, malonamide **3a**, sterically hindered at the acyl region extracted slightly higher amounts of Ag^+ compared to **1a** attributed to the higher solubility of the Ag^+ -**3a** complex in chloroform than the Ag^+ -**1a** complex (**1a** = 96.3 ± 1.2 % versus **3a** = 98.9 ± 0.2 %). It is worth noting that the ligand **3a** extracted slightly higher amounts of Ag^+ than the ligand **1i**, attributed to the location of steric hindrance away from the crucial sulfur donor centre as earlier explained. Interestingly both **1i** and **3a** were less selective than **1a** for binding with Pb^{2+} (**1i** $K_{\text{Ag}^+/\text{Pb}^{2+}} = 4.5$, **3a** $K_{\text{Ag}^+/\text{Pb}^{2+}} = 11.1$, **1a** $K_{\text{Ag}^+/\text{Pb}^{2+}} = 321$) and this could be attributed to the higher solubility of all the malonamide- Pb^{2+} complexes in chloroform due to the gem dialkyl groupings.[17]

Investigation of Ag^+ -malonamide derivative **1a** binding stoichiometry

Mass spectrometry studies

To gain insight into the nature of the binding of Ag^+ by the malonamide derived ligands, Ag^+ complexes of **1a**, were prepared by varying the equivalents of the silver salt (1-3 eq) relative to the ligand. Consequently, the Ag^+ -**1a** complexes (**4a-c**) were obtained in moderate to high yields (Table 2) and characterized by means of low- and high-resolution mass spectrometry. In the wide scan (m/z 0 – 2400) low resolution mass spectrometry (LRMS) of **4a**, the only pair of peaks with ratio of ~1:1 (indicative of a Ag^+ complex) were observed at m/z 509 and 511 (Figure 6). Indeed, the m/z 509 was confirmed by high resolution mass spectrometry (HRMS) analyses as the complex - [$^{107}\text{Ag}(\mathbf{1a})$] $^+$ (found: 509.0481, calculated: 509.0487). Interestingly, reacting the ligand **1a** with 2 equivalents and 3 equivalents of silver triflate gave **4b** and **4c** respectively (Entries 2 and 3, Table 2) which were also both found, after LRMS analyses to be Ag^+ -**1a** complexes with a 1:1 stoichiometry. These results indicate that the stoichiometry of the Ag^+ complex with malonamide **1a** is perhaps 1:1.

Table 2. Effect of Ag^+ equivalent on stoichiometry of Ag^+ complexes of **1a** and silver triflate

Entry	Ligand	$\text{AgOSO}_2\text{CF}_3$ eq.	Product	$\text{Ag}^+:\mathbf{1a}$	Yield
1	1a	1	4a	1:1	91 %
2	1a	2	4b	1:1	65 %
3	1a	3	4c	1:1	85 %

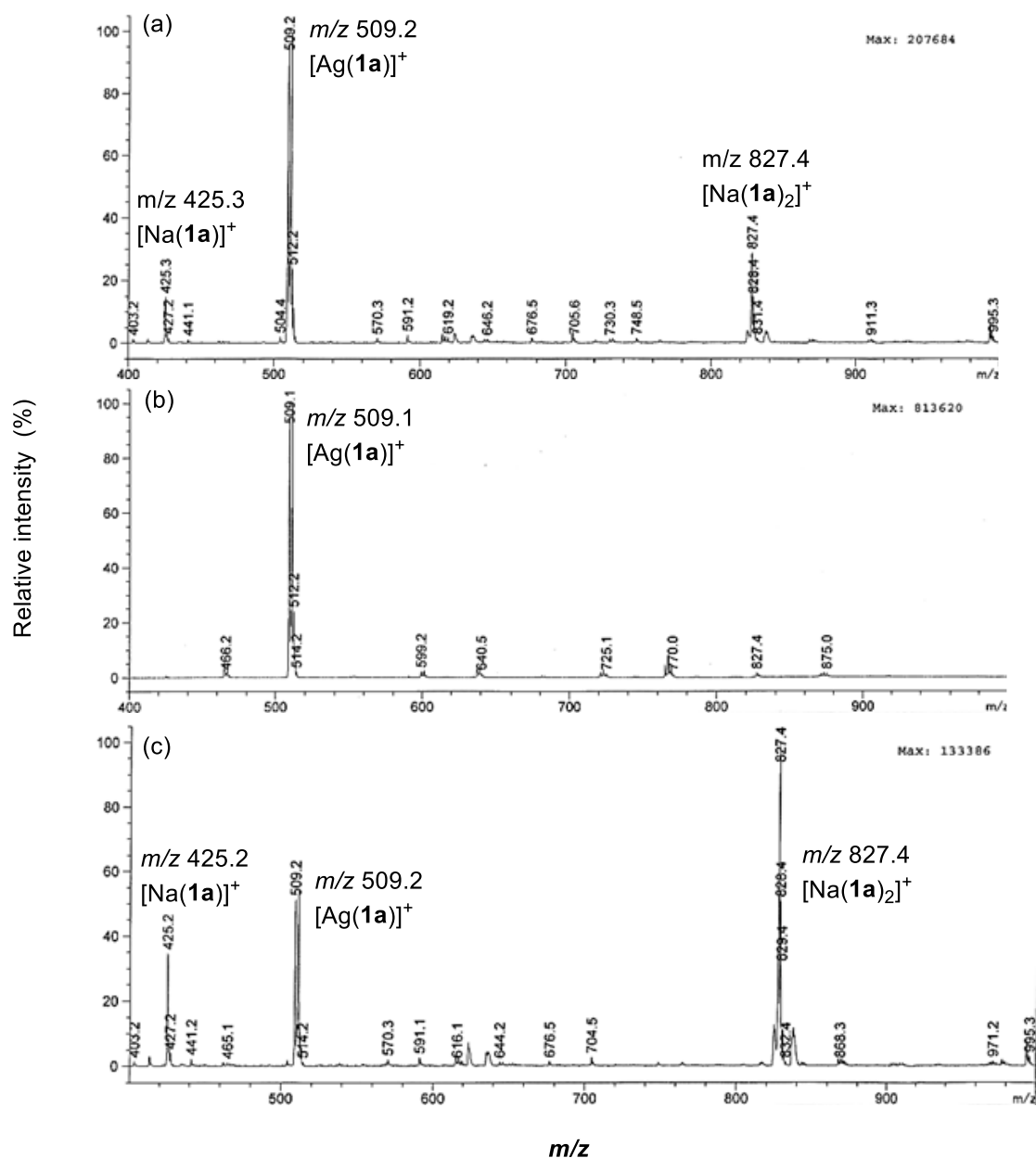


Figure 6. Partial low-resolution ESI mass spectra of Ag^+ -**1a** complexes from treatment of **1a** with (a) one (b) two and (c) three equivalents of $\text{AgOSO}_2\text{CF}_3$

Proton NMR studies - Job's plot and mole ratio

The Job's plot for the Ag^+ -**1a** perchlorate complex was constructed from ^1H NMR titration of equal concentrations (0.005 M) of ligand **1a** against AgClO_4 . The ^1H NMR titration of the Ag^+ against the ligand **1a** was undertaken in DMSO-d_6 after initial solvent screening experiments revealed the unsuitability of other common NMR solvents tested (due to poor solubility of the ligand **1a**). The ^1H NMR titrations of Ag^+ against **1a** did not lead to the appearance of new peaks (Figure 7a) but caused

distinct changes in chemical shifts, indicating a fast rate of Ag^+ exchange between the complexed and uncomplexed states. The Job's plot for the interaction of Ag^+ with **1a** (Figure 7b) was constructed after appropriate calculations had been undertaken. The gentle curvature of the curves in the Job's plot (Figure 7b) indicates the binding between the ligand **1a** and Ag^+ is perhaps weak.[20] Furthermore, it can be observed that the coefficient on the x-axis of the maxima of all curves in the Job's plot is at $\chi_{\text{Ag}^+} = 0.5$, indicating that the malonamide **1a** bind Ag^+ in any of the 1:1, 2:2 or any other $n:n$ fashion. To confirm the actual stoichiometry, a different ^1H NMR titration of the interaction of **1a** with Ag^+ were constructed towards generating a mole ratio plot. Therefore, a constant amount of a 0.539 M Ag^+ solution was successively added to the ligand **1a** solution to prepare $\text{Ag}^+/\mathbf{1a}$ mole ratios ranging from 0.5 to 4.0. Proton NMR spectra after successive addition of the Ag^+ solution were recorded (Figure 7c), and the mole ratio plot was constructed from the values obtained (Figure 7d). In a typical mole ratio plot, the stoichiometry of a complex is the coefficient on the x-axis of the point of inflection. The point of inflection is the point on a curve where the shape of the curve changes. In the case of the $\text{Ag}^+ \text{-} \mathbf{1a}$ complex (Figure 7d), it was very difficult to get a distinct point of inflection for any of the curves, indicating a weak binding between the Ag^+ and **1a** and confirming the observation from the Job's plot.[20] It also suggests that the $\text{Ag}^+ \text{-} \mathbf{1a}$ complex may be adopting more than one type of stoichiometry in solution including the 1:1 observed from mass spectrometry and the Job's plot.

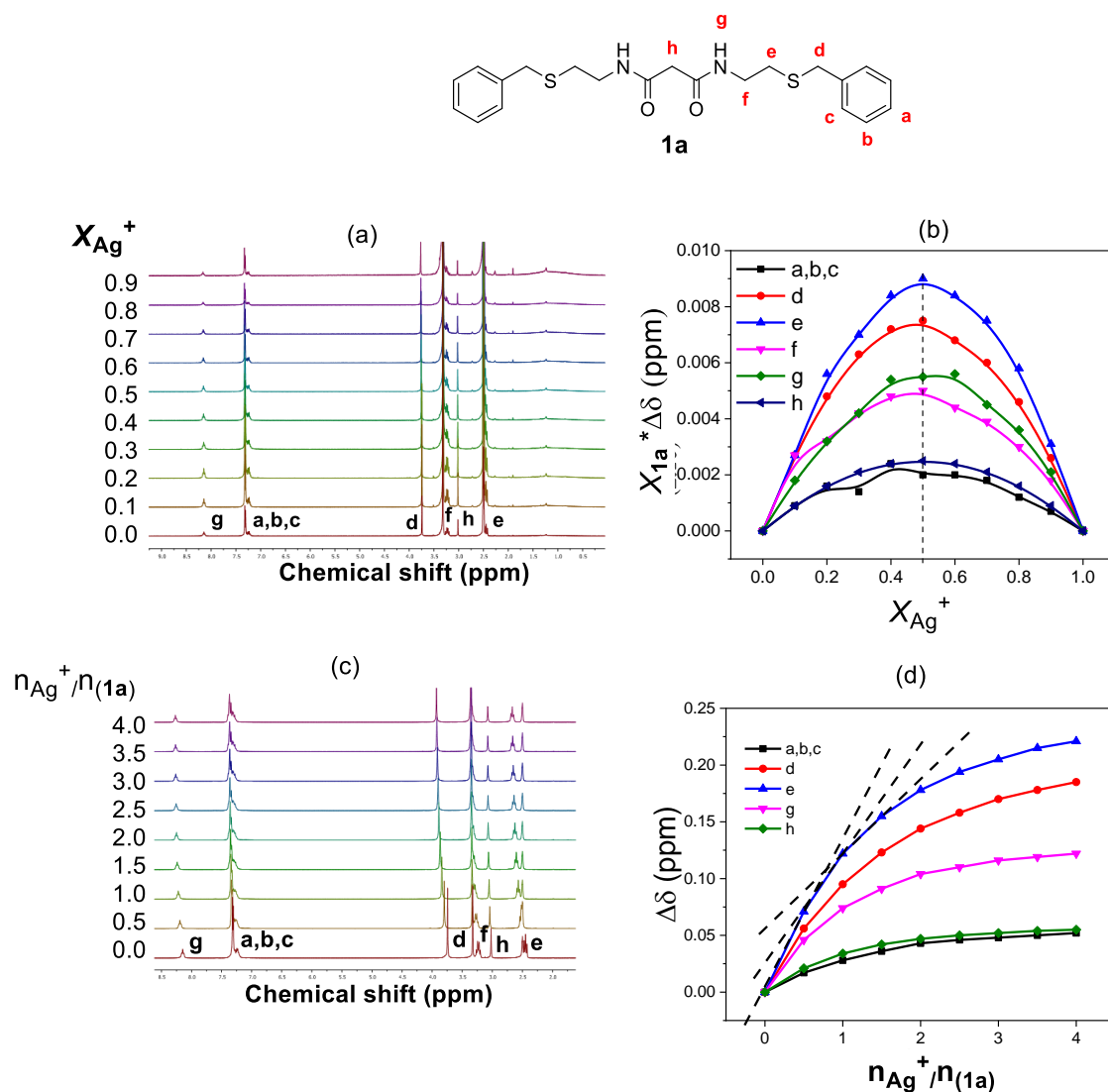


Figure 7. (a and c) ¹H NMR (300 MHz) spectra of the interaction of Ag⁺ with **1a**, (b) Job's and (d) mole ratio plots of the interaction of Ag⁺ with ligand **1a**.

In the Job's plot (Figure 7b), the highest $\Delta\delta$ values were observed for protons 'e' and 'd' in **1a** (the protons on carbons alpha to the *S*- donor atoms). The next highest $\Delta\delta$ values were observed for protons 'g' in **1a** (the amide protons). The observed high $\Delta\delta$'s may be due to deshielding effects experienced by these protons as the *S*- and *N*- donors participate in binding Ag⁺. Unsurprisingly, lower $\Delta\delta$ values were observed for phenyl protons ('a', 'b' and 'c' in **1a**) since they are not in the neighbourhood of the *S*- and *N*- donors (Figures 7b). Based on these observations, it was hypothesized that the ligand **1a** binds Ag⁺ using its two *S*- and *N*- donor centres to form a tetrahedral complex (Figure 8).

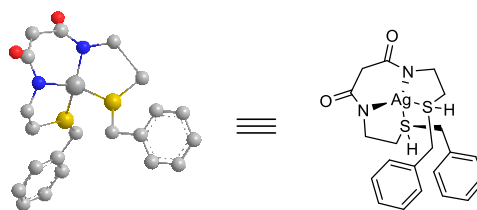


Figure 8. Proposed structure for $[\text{Ag}(\mathbf{1a})]^+$

Conclusion

A novel room temperature route to access a range of malonamide derivatives **1a** and **1e-i** in moderate to high yields has been reported. Also, gem diethyl substituted derivatives of **1a** (**3a-e**) were also prepared. Electronic effects at the 4-position of the aromatic groups in the malonamides **1e-h** had little effect on Ag^+ extraction efficiency but a great effect on metal selectivity, with the electron rich (4-methoxy) malonamide **1f** being the most selective for Ag^+ over Cu^{2+} and Pb^{2+} . Steric hindrance near the sulphur atom has a small negative effect on Ag^+ extraction efficiency, while hindrance at the central carbon atom lowers selectivity. The binding stoichiometries of the Ag^+ complexes of the ligand **1a** were determined by mass spectrometry, Job's and mole ratio plots (from ^1H NMR titrations) and observed to be a 1:1 type, leading to the predication that **1a** binds Ag^+ in a tetrahedral fashion. We have therefore shown that by simple modification of the electronics and sterics of the *N,N'*-bis(2-(benzylthio)ethyl)malonamides, their selectivity for Ag^+ recovery from aqueous solutions can be improved over **1a**.

Acknowledgments

The authors would like to thank The Commonwealth Scholarship Commission in the United Kingdom and The University of Warwick for funding Abiodun's PhD.

Declaration of interest statement

The authors declare no conflict of interest.

References

- [1] Sahan M, Kucuker MA, Demirel B, et al. Determination of Metal Content of Waste Mobile Phones and Estimation of Their Recovery Potential in Turkey. *Int J Environ Res Public Health*; 16. Epub ahead of print 1 March 2019. DOI: 10.3390/ijerph16050887.
- [2] Taillades G, Sarradin J. Silver: High performance anode for thin film lithium ion batteries. *J Power Sources* 2004; 125: 199–205.
- [3] Buttermann BWC, Hilliard HE. *Mineral Commodity Profiles: Silver*. Virginia, 2005. Epub

- ahead of print 2005. DOI: <https://pubs.usgs.gov/of/2004/1251/2004-1251.pdf>.
- [4] Kolpakova N, Sabitova Z, Sachkov V, et al. Determination of Au(III) and Ag(I) in Carbonaceous Shales and Pyrites by Stripping Voltammetry. *Minerals* 2019; 9: 78.
- [5] Avarmaa K, Klemettinen L, O'Brien H, et al. Urban mining of precious metals via oxidizing copper smelting. *Miner Eng* 2019; 133: 95–102.
- [6] Jańczewski D, Reinhoudt DN, Verboom W, et al. Tripodal (N-alkylated) CMP(O) and malonamide ligands: Synthesis, extraction of metal ions, and potentiometric studies. *New J Chem* 2007; 31: 109–120.
- [7] Patil AB, Pathak PN, Shinde VS, et al. Synthesis and Evaluation of N,N'-dimethyl-N,N'-dicyclohexyl-Malonamide (DMDCMA) as an Extractant for Actinides. *Sep Sci Technol* 2014; 49: 2927–2932.
- [8] Manchanda VK, Pathak PN. Amides and diamides as promising extractants in the back end of the nuclear fuel cycle: An overview. *Separation and Purification Technology* 2004; 35: 85–103.
- [9] Daubinet A, Kaye PT. Designer ligands. VIII. Thermal and microwave-assisted synthesis of silver(I)-selective ligands. *Synth Commun* 2002; 32: 3207.
- [10] Ghosh S, Tochtrop GP. A new strategy for the synthesis of -benzylmercaptoethylamine derivatives. *Tetrahedron Lett* 2009; 50: 1723–1726.
- [11] Carroll FI, White JD, Wall ME. Organic Sulfur Compounds. I. Synthesis of sec-Mercaptoalkylamine Hydrochlorides 1a,b. *J Org Chem* 1963; 28: 1236–1239.
- [12] Daubinet A. *Design, synthesis and evaluation of silver-specific ligands*. Rhodes University, 2001.
- [13] Sole KC, Hiskey JB. Solvent extraction characteristics of thiosubstituted organophosphinic acid extractants. *Hydrometallurgy* 1992; 30: 345–365.
- [14] Toure M, Arrachart G, Duhamet J, et al. Tantalum and Niobium Selective Extraction by Alkyl-Acetophenone. *Metals (Basel)* 2018; 8: 654.
- [15] Fielding L. Determination of Association Constants (Ka) from Solution NMR data. *Tetrahedron* 2000; 56: 6151–6170.
- [16] Crane RA, Sinnott DE, Cleall PJ, et al. Physicochemical composition of wastes and co-located environmental designations at legacy mine sites in the south west of England and Wales: Implications for their resource potential. *Resour Conserv Recycl* 2017; 123: 117–134.

- [17] Ocak Ü, Alp H, Gökçe P, et al. The synthesis of new *N2,S2* -Macrocyclic schiff base ligands and investigation of their ion extraction capability from aqueous media. *Sep Sci Technol* 2006; 41: 391–401.
- [18] Pearson RG. Hard and soft acids and bases, HSAB, part 1: Fundamental principles. *J Chem Educ* 1968; 45: 581.
- [19] Hiruta Y, Watanabe T, Nakamura E, et al. Steric hindrance effects in tripodal ligands for extraction and back-extraction of Ag^+ . *RSC Adv* 2014; 4: 9791–9798.
- [20] Renny JS, Tomasevich LL, Tallmadge EH, et al. Method of continuous variations: Applications of job plots to the study of molecular associations in organometallic chemistry. *Angew Chemie - Int Ed* 2013; 52: 11998–12013.